

Palladium(II) complex induces apoptosis through ROS-mediated mitochondrial pathway in human lung adenocarcinoma cell line (A549)

Tarun Keswani¹, Santanu Chowdhury²,
Soma Mukherjee² and Arindam Bhattacharyya^{1,*}

¹Immunology Lab, Department of Zoology, University of Calcutta,
35, Ballygunge Circular Road, Kolkata 700 019, India

²Department of Environmental Science, University of Kalyani,
Nadia 741 235, India

Treatment for lung cancer is still far from satisfactory. Therefore, there is a call for novel anticancer agents. In the present study, the anticancer activity of [Pd(L)Cl], 1a complex towards A549 human lung adenocarcinoma cells was investigated. [Pd(L)Cl], 1a inhibited the growth of A549 cells in a time and dose-dependent manner. The IC₅₀ value was 10 μ M after 24 h treatment. Flow cytometric analyses revealed a dose-related increase in the percentages of cells in the Sub-G₀/G₁ state, indicative of apoptosis which was further confirmed by Annexin V binding assay, via a ROS-mediated mitochondria-dependent pathway. Western blot analysis showed that 1a complex induced Bax expression to desintegrate the outer mitochondrial membrane and causing cytochrome *c* release, associated with the activation of caspase-3. All of these signal transduction pathways are involved in initiating apoptosis. [Pd(L)Cl], 1a seems to represent a potentially active drug against non-small cell lung cancer A549 cell line *in vitro*, and further studies *in vivo* are warranted.

Keywords: Apoptosis, lung cancer, palladium(II) complexes, reactive oxygen species.

LUNG cancer is one of the most common-disease causing death worldwide¹. Although many drugs have been introduced into the market, response to therapy is still poor. The foremost target of most research groups is to find a convenient anti-cancer drug that can be used efficiently for the treatment of human tumours. The recent history of metal-containing antitumour agents began with the unexpected detection of antitumour properties for inorganic compound *cis*-diamminedichloroplatinum(II) (cisplatin) in 1969 (ref. 2). It seemed that such biological activity had to be unique among heavy metal compounds and was seen as a result of the definite kinetic and structural properties at platinum(II) centre, making possible the specific impact on genomic DNA. There is steadily a growing interest in investigations of transition metal complexes other than the traditional platinum-based compounds for use as chemotherapeutic agents against cancer.

Current metal-based drugs research is moving towards the development of new agents which are able to improve effectiveness and reduce the severe side effects of *cis*-diammine-dichloroplatinum(II) (cisplatin) and its analogues that are still the most widely used anti-cancer therapeutics³. Along with platinum(II) complexes, numerous planar and octahedral platinum complexes as well as compounds of other platinum-group metals such as ruthenium, rhodium or palladium were characterized by cytostatic activity⁴⁻⁶. The major classes of metal-based anticancer drugs include platinum(II), palladium(II), gold(I), gold(III), metaloporphyrins, ruthenium(II), ruthenium(III), bismuth(III) and copper(II) compounds. Special attention in this regard has been given to palladium(II) complexes⁷⁻¹¹, since the coordination pattern and complexation behaviour of palladium(II) are similar to those of platinum(II)^{7,12,13}. However, platinum(II) complexes are thermodynamically and kinetically more stable than those of palladium(II). The complexes undergo equilibrium and ligand exchange reactions 10⁵ times faster than the corresponding platinum(II) analogues. Importantly, a good relationship was observed between the cytostatic activity of the palladium(II) complexes and their lipophilicity or solubility¹⁴. As non-platinum complexes, they have recently been reviewed to have a significant anti-tumour activity to cancer cells as well as lower side effects compared to cisplatin¹⁵, this often-used chemotherapeutic in clinics.

As an important feature of metal-containing anti-cancer agents, palladium(II) complexes are expected to have less kidney toxicity than cisplatin¹⁶. Moreover, better solubility compared to platinum(II) seems to make palladium(II) complexes more attractive. In one study, palladium(II) complexes of glyoxylic oxime were found to have higher aqueous solubility than platinum(II) complexes of glyoxylic oxime¹⁷. The palladium(II) complexes dissociate readily in solution leading to very reactive species that are unable to reach their pharmacological targets such as DNA^{7,18,19}. This rapid aquation and formation of very reactive species could be overcome if palladium(II) complexes are stabilized by bulky ligands and suitable leaving groups⁷. As a result, a number of palladium(II) complexes with neutral ligands have shown promising results. Palladium complexes with 1-benzyl-3-tert-butylimidazol-2-ylidene, which are active against tumour cells, have an antiproliferative activity stronger than cisplatin²⁰. Palladium(II) complexes derived from thiosemicarbazones are active against cisplatin-resistant cell lines⁹, while benzaldehyde thiosemicarbazones²¹ exhibit cytotoxicity against human tumour (carcinoma, melanoma and leukaemia) cell lines. The literature also describes the anti-proliferative activity of palladacycles²², a large variety of palladium complexes containing triphenylphosphine and thymidine moiety²³, pyrazole ligands²⁴ and methionine sulphoxide²⁵.

Palladium complexes with two different chelating ligands, tropolone and bipyridine, have also been

*For correspondence. (e-mail: arindam19@yahoo.com)

reported, their biological evaluation revealing activity *in vitro* against human tumour cells lines^{26,27}. The success of metallo drugs is closely linked with the proper choice of ligands, as they play a crucial role in modifying reactivity and lipophilicity, stabilizing specific oxidation states, imparting substitution inertness²⁰ and influencing metal coordination pattern. Recent research has been directed towards synthesis and evaluation of complexes with biologically interesting ligands with the aim of widening the spectrum of complex activity^{7,19,28}. In the present work, we have investigated the anti-cancer activity of a novel palladium(II) complex. A luminescent palladium(II) complex [Pd^{II}(L)Cl], **1a** with the acyclic tridentate quinoline-2-carboxaldehyde-2-pyridylhydrazone ligand, HL, **1**, was previously synthesized²⁹. We have further investigated the anti-proliferative activity and the capacity to induce apoptosis of the novel complex **1a** against human lung cancer cell line, A549.

Stock solution of the previously synthesized²⁹ [Pd^{II}(L)Cl], **1a** complex was prepared in DMSO (Sigma-Aldrich, USA) at a concentration of 20 mM, filtered through a Millipore filter (0.22 μ M), before treatment, and diluted with culture medium to at least six different working concentrations ranging from 0 to 25 μ M. Culture medium was DMEM supplemented with 10% foetal bovine serum (Himedia) and antibiotics/antimycotic (conc. 100 units) and gentamycin (conc. 50 μ g/ml) solution with Na-pyruvate (1 mM). Human lung cancer cell line A549 was purchased from the National Centre for Cell Science, Pune, and cultured in DMEM supplemented with 10% FBS and antibiotics/antimycotic (conc. 100 units) and gentamycin (conc. 50 μ g/ml) solution with Na-pyruvate (1 mM) in a humidified incubator at 37°C in 5% CO₂.

A549 cells (50,000 cells/cm²) were seeded in triplicate into six-well plates for 24 h. Then the cells were supplemented with different concentrations of [Pd^{II}(L)Cl], **1a** for 24 h. Cell viability was measured by trypan blue dye exclusion method. DMSO was used as negative control and cisplatin was used as reference drug. After 24 h, 1.0 $\times 10^6$ ml⁻¹ cell suspension for viability assay was prepared by trypsinization, centrifugation and counting with a haemocytometer. A 1 : 1 dilution of 200 μ l of the cell suspension was made using 0.4% trypan blue solution and incubated for 3 min at room temperature. Replicate samples of stained and unstained cells from each well were counted with a haemocytometer on a microscope under a 20 \times objective. Following analysis of variance, data from all experiments were pooled for further statistical analysis. The calculated percentage of unstained cells represents the percentage of viable cells.

For cell cycle distribution, A549 cells were seeded in growth medium in six-well plates (3 $\times 10^5$ per well) and grown overnight at 37°C in a humidified incubator with 5% CO₂. Cells were then treated with [Pd^{II}(L)Cl], **1a** at indicated concentrations for 24 h. Cell-cycle analysis was

performed as described earlier²⁹. The propidium iodide (PI) fluorescence was then measured using a FL-2 filter (585 nm) in a BD FACS Calibur flow cytometer (Becton Dickinson); a minimum of 10,000 events were acquired for each sample. The flow cytometric data were ultimately analysed using WinMDI 2.9 and histogram display of DNA content (*X*-axis, PI-fluorescence) versus counts (*Y*-axis) was displayed.

Early apoptotic process is characterized by changes in the phospholipid bilayers of cell membranes. Staining with FITC-conjugated annexin V and PI can help quantify subpopulations of cells with compromised membrane integrity. Untreated control and 5 and 10 μ M of [Pd^{II}(L)Cl], **1a** treated cells were washed twice with cold PBS and resuspended in buffer at a concentration of 1.0 $\times 10^6$ per ml. Cells were mixed with 1 μ l of fluorescein isothiocyanate (FITC)-conjugated annexin V reagent (BioVision, USA) and PI solution (conc. 10 μ g/ml). After 15 min incubation at room temperature in the dark and further washing, the samples were analysed by flow cytometry. Cells were then analysed in the FACS Calibur flow cytometer; for each sample, a minimum of 10,000 events was acquired. Using WinMDI 2.9 software, histogram displays of DNA content (*X*-axis, PI-fluorescence) versus counts (*Y*-axis) were generated. Cells that were positive for both PI and annexin V were considered as necrotic cells and thus excluded from analysis. All results were expressed as the percentage of apoptotic cells (\pm SD)/sample.

The generation of reactive oxygen species (ROS) was detected by DCFDA fluorescence. Intracellular, membrane-bound esterases and ROS respectively, cleave and oxidize non-fluorescent H₂DCFDA to the fluorescent 2',7'-dichlorofluorescein (DCF). Cells were seeded (4.0 $\times 10^5$ cells/well) in six-well plates and allowed to adhere overnight. The cells were then treated with [Pd^{II}(L)Cl], **1a** concentrations of 0, 5.0 and 10.0 μ M for 24 h at 37°C. The treated cells were incubated with 100 μ M final concentration of DCFDA for 35 min in the dark at 37°C. The cells were harvested by centrifugation at 1500 rpm for 3–5 min, resuspended in phosphate buffered saline (PBS), and ROS generation of 10,000 cells was measured by the fluorescence intensity (FL-1, 530 nm). Logarithmic amplification was used to detect the fluorescence of the probe. Four independent experiments were performed in triplicate. Data were analysed using WinMDI 2.9, and they represent the mean fluorescence intensity.

Loss of mitochondrial transmembrane potential ($\Delta\psi_m$) was determined by the retention of the dye DiOC₆. A549 cells were seeded (4.0 $\times 10^5$ cells/well) in six-well plates and then treated with [Pd^{II}(L)Cl], **1a** concentrations of 5.0 and 10.0 μ M for 24 h at 37°C. After 24 h cells were harvested and washed with PBS, incubated with 100 nM DiOC₆ at 37°C for 30 min in the dark. Loss of DiOC₆ fluorescence indicates disruption of the mitochondrial inner transmembrane potential. The probe was excited at

488 nm and emission was measured through a 530 nm band pass filter. Logarithmic amplification was used to detect the fluorescence of the probe. Data were analysed using WinMDI 2.9, and they represent the mean fluorescence intensity.

A549 cell death induced by the studied compounds was analysed by observing the change of nuclear morphology stained with acridine orange (AO). When AO enters into the cells, it shows green colour. Also, 4.0×10^5 of A549 cells were seeded on the six-well culture plates. Following 24 h incubation 5.0 and 10 μM concentration of the studied compound was added to the cells. After 24 h of treatment, cells were washed with PBS and fixed with 4% paraformaldehyde solution for 15 min. Cell were stained with 5 $\mu\text{g}/\text{ml}$ AO for 5 min. The cells were observed and photographed under an Olympus Bx51 fluorescence microscope.

For immunofluorescence of Bax, A549 cells were grown in poly-L-lysine (0.1 mg/ml) coated sterile cover slip. Cells were treated with or without the presence of 5.0 and 10 μM concentration of $[\text{Pd}^{\text{II}}(\text{L})\text{Cl}]$, **1a** complex for 24 h. After washing three times with PBS, coverslips were fixed with 4% paraformaldehyde for 15 min at room temperature. Cells were permeabilized with PBS containing 0.1% Triton X-100 for 5 min and then washed three times with PBS. After blocking with 3% BSA in TBS solution for 1 h, the cells were incubated with monoclonal antibody of anti-Bax (1 : 100) overnight. After completion of primary antibody incubation, the cells were incubated for 2 h with a dilution 1 : 100 of goat anti-mouse FITC conjugated secondary antibody. Finally, the nucleus was stained with 1 $\mu\text{g}/\text{ml}$ DAPI (4,6 diamidino-2-phenylindole) for 5 min. Images were collected by an Olympus BX51 fluorescence microscope provided with a cool-snap digital camera. Filters used were: 460–490 nm excitation and 510–550 nm emission for FITC; 360–370 nm excitation and 420–460 nm emission for DAPI.

After washing in cold PBS, 9×10^6 cells/90 mm petri dishes, the cells were lysed using the lysis buffer (150 mM sodium chloride, 1.0% Triton X-100, 50 mM Tris pH 8.0, 0.01% SDS, 0.5% sodium deoxycholate) containing 1 mM PMSF, aprotinin 1 $\mu\text{g}/\text{ml}$ and leupeptin 1 $\mu\text{g}/\text{ml}$. Supernatants were collected by centrifugation at a 14,000 rpm for 15 min at 4°C. Then protein estimation was done using the Bradford method at 595 nm. For Western blot analysis of cytochrome *c* and caspase-3, the cell lysate (40 μg) was loaded onto a 10–15% sodium dodecyl sulphate polyacrylamide gel after electrophoresis; separated proteins were transferred onto nitrocellulose membrane (Millipore, Bedford, MA). The membrane was blocked in 5% nonfat dry milk and blotted with primary antibodies diluted in a blocking solution (5% BSA in TBS). After washing, the membrane was incubated with AP-conjugated secondary antibodies according to the manufacturer's instructions. Positive reactions were visualized using the developer NBT and BCIP solution. Western blot and

densitometry studies were performed using Bio-Rad Gel Documentation system. β -actin was also analysed on each membrane for confirmation of gel sample loading (i.e. based on constitutive expression).

Data obtained from experiments are represented as mean \pm SD of at least three independent determinations. One-way analysis of variance was applied to determine the possible significant differences followed by Student's *t*-test and *P* value ≤ 0.05 was considered as statistically significant difference.

The effects of $[\text{Pd}^{\text{II}}(\text{L})\text{Cl}]$, **1a** complex on A549 cells were first evaluated by trypan blue exclusion assay, which indicated that the **1a** complex significantly decreases the percentage of viable A549 cells in a dose-dependent manner. As shown in Figure 1 *a*, the viable cells at 24 h after treatment with $[\text{Pd}^{\text{II}}(\text{L})\text{Cl}]$, **1a** complex decreased to 64% (5 μM), 50% (10 μM) and 18% (25 μM) with respect to the control. The trypan blue assay showed that IC_{50} is 10 μM for **1a** complex (Figure 1 *a*). Simultaneously to determine the cytotoxic effects of $[\text{Pd}^{\text{II}}(\text{L})\text{Cl}]$, **1a** on A549 cells, we observed the alterations in cell morphology. The results showed that $[\text{Pd}^{\text{II}}(\text{L})\text{Cl}]$, **1a** led to apparent morphological changes in a dose-dependent manner. The conspicuous changes observed in $[\text{Pd}^{\text{II}}(\text{L})\text{Cl}]$, **1a** treated cells included cell shrinkage,

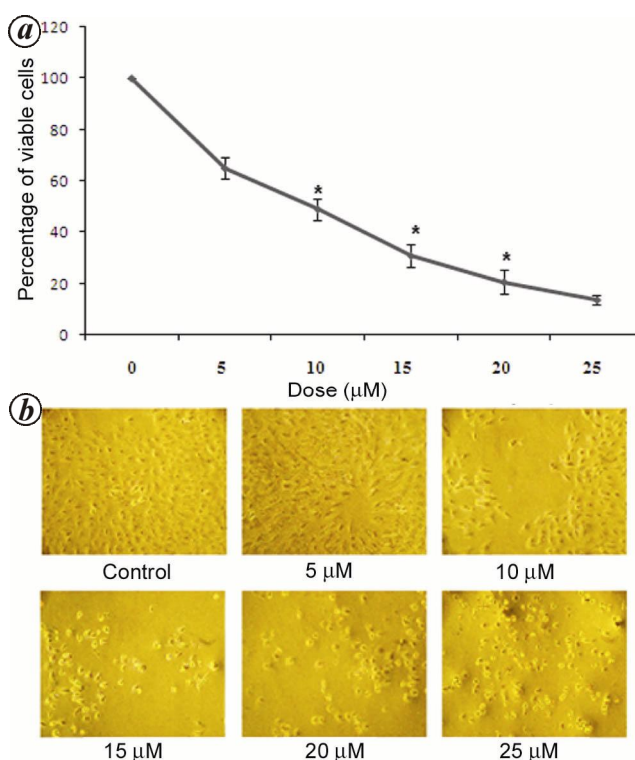


Figure 1. Cytotoxic effects of $[\text{Pd}^{\text{II}}(\text{L})\text{Cl}]$, **1a** on A549 cells. *a*, Inhibitory effects of $[\text{Pd}^{\text{II}}(\text{L})\text{Cl}]$, **1a** on the cell viability of A549 cells by trypan blue exclusion assay. *b*, Cell morphology under light microscopy after incubation with $[\text{Pd}^{\text{II}}(\text{L})\text{Cl}]$, **1a** at indicated concentrations for 24 h (magnification 20 \times). Data are presented as mean \pm SD by three independent experiments. Significance: **P* < 0.05 versus control.

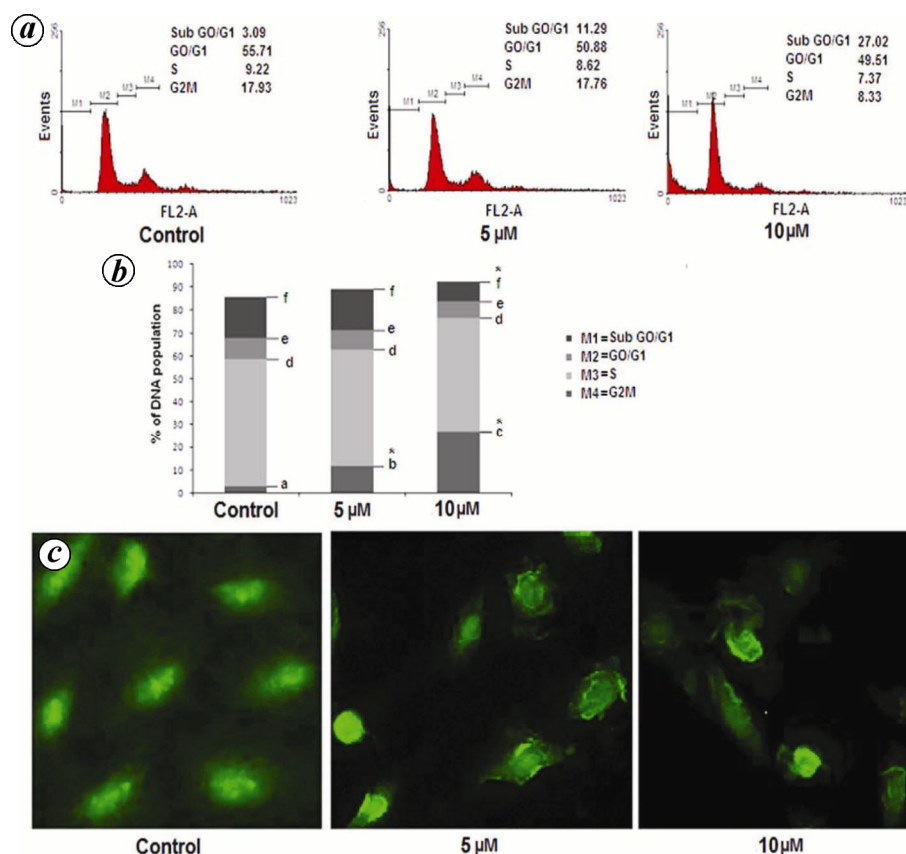


Figure 2. Flow cytometric analysis of $[\text{Pd}^{\text{II}}(\text{L})\text{Cl}]_1\mathbf{a}$ induced cell cycle arrest in A549 cells. **a**, Cells were harvested and processed for cell cycle analysis using propidium iodide. Cell cycle phase distribution of A549 nuclear DNA was determined by single label flow cytometry. Histogram display of DNA content (X-axis, PI fluorescence) versus counts (Y-axis) has shown (Sub G0/G1, G0/G1, S, G2/M): 0, 5 and 10 μM $[\text{Pd}^{\text{II}}(\text{L})\text{Cl}]_1\mathbf{a}$ after 24 h treatment. **b**, Bar represents the percentage of A549 cells DNA population in different stages of cell cycle after $[\text{Pd}^{\text{II}}(\text{L})\text{Cl}]_1\mathbf{a}$ treatment. Results are a single representative of five comparable experiments. Asterisks (*) indicates significant differences ($P < 0.05$, ANOVA followed by post hoc LSD test) in values for different doses compared to controls. The different letters indicate significant differences ($P < 0.05$) between groups. **(c)** Morphological changes of cell apoptosis detected by acridine orange staining. 0, 5 and 10 μM of complex treated A549 cell condensed nucleus (magnification 40 \times). Data are presented as the best representative of five independent experiments.

round-up and extensive detachment of the cells from the culture substratum. These changes became increasingly visible with dose increase, but were absent in the control cells (Figure 1 *b*).

To determine whether or not $[\text{Pd}^{\text{II}}(\text{L})\text{Cl}]_1\mathbf{a}$ complex exerted its cytotoxic effect via the induction of cell cycle arrest or apoptosis, we examined the distribution of cell cycles of A549 cells by flow cytometry, after their exposure to $[\text{Pd}^{\text{II}}(\text{L})\text{Cl}]_1\mathbf{a}$ complex. As shown in Figure 2 *a*, $[\text{Pd}^{\text{II}}(\text{L})\text{Cl}]_1\mathbf{a}$ complex induced an altered cell cycle distribution in a dose-dependent manner. The flow cytometry data revealed a dose-related substantive increase in the percentages of cells at sub-G0/G1 (might be apoptotic cells; M1) after 5 μM (i.e. 3–4-fold) and 10 μM (i.e. 8–9 fold) $[\text{Pd}^{\text{II}}(\text{L})\text{Cl}]_1\mathbf{a}$ treatment respectively, compared to control cells. The percentages of cells at G0/G1 phase at 24 h after treatment with $[\text{Pd}^{\text{II}}(\text{L})\text{Cl}]_1\mathbf{a}$ complex (5 and 10 μM) did not significantly decrease (Figure 2 *a* and *b*).

For further confirmation of apoptosis in A549 cells, the change in nuclear morphology by AO staining and annexin V staining before and after $[\text{Pd}^{\text{II}}(\text{L})\text{Cl}]_1\mathbf{a}$ complex treatment was observed. After AO staining the nuclei of the control cells were round and homogeneous, whereas after $[\text{Pd}^{\text{II}}(\text{L})\text{Cl}]_1\mathbf{a}$ complex treatment a reduction of cell volume, nuclear condensation (a hallmark of apoptotic cells), and increased non-adherence of the cells to the culture surface (Figure 2 *c*) were observed. Induction of apoptosis was rigorously substantiated by examining the flow cytometry pattern of annexin V-FITC stained cells (Figure 3 *a*). It was found that the number of annexin V + PI⁺, i.e. early apoptotic cells, increases significantly in 5 (~15.0%) and 10 μM (~25.0%) compared to the untreated cells (~0.5%) and number of annexin V⁺/PI⁺, i.e. late apoptotic cells also increases in 10 μM (~5.0%) compared with the untreated one (0.1%; Figure 3 *a* and *b*).

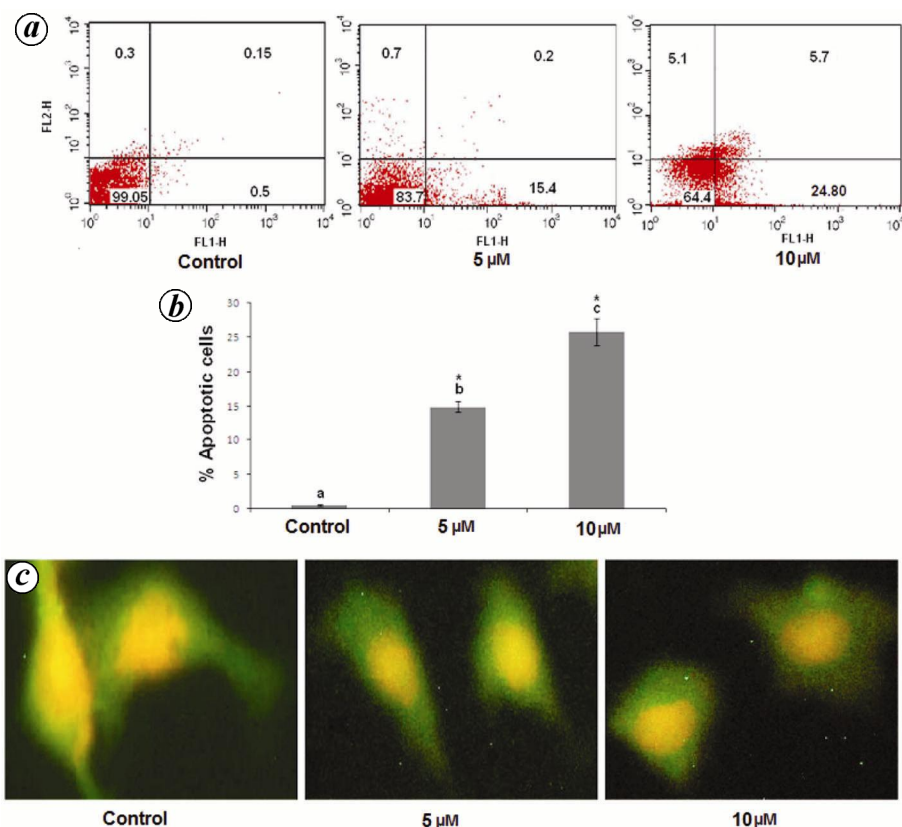


Figure 3. Flow cytometric analysis of apoptotic cells after treatment of A549 cells with $[\text{Pd}^{\text{II}}(\text{L})\text{Cl}]$, **1a**. The cells were harvested and labelled with annexin-V-FITC and PI and analysed by flow cytometry. **a**, Representative biparametric histograms obtained after 24 h of incubation at the indicated concentration of 0, 5 and 10 μM $[\text{Pd}^{\text{II}}(\text{L})\text{Cl}]$. The lower left-hand segment represents the annexin-V⁻/PI⁻ cells, the lower right-hand segment the annexin-V⁺/PI⁻ cells, the upper right-hand segment the annexin-V⁺/PI⁺ cells, and the upper left-hand segment the annexin-V⁻/PI⁺ cells. **b**, Bar graph represents the percentage of apoptotic population at different treatment conditions. Results are the best representative of five comparable experiments. Asterisks (*) indicates significant differences ($P < 0.05$, ANOVA followed by post hoc LSD test) in values for different doses compared to control. The different letters indicate significant differences ($P < 0.05$) between groups. **c**, Immunofluorescent assay of pro-apoptotic protein. Immunofluorescent analysis of the expression of Bax (green). The cells were incubated with anti-Bax, antibody followed by incubation in appropriate fluorescent secondary antibody. Nuclei were stained with ethidium bromide (red) for 5 min. The images were photographed under an Olympus fluorescence microscope (magnification 100 \times). Data are presented as the best representative of five independent experiments.

It has been reported that activation of the proapoptotic Bcl-2 family members, Bax (or Bak), is an essential gateway to mitochondrial dysfunction required for cell death induced by diverse cytotoxic stress. Therefore, here we have studied the expression of Bax by immunofluorescence staining. A549 cells were exposed to 5 and 10 μM concentration of $[\text{Pd}^{\text{II}}(\text{L})\text{Cl}]$ complex along with a control and the localization of Bax was investigated within cytosol using FITC-conjugated secondary antibody, which gives the green fluorescence and as a counter stain the nucleus was stained by ethidium bromide. Expression of Bax increased with the treatment of the $[\text{Pd}^{\text{II}}(\text{L})\text{Cl}]$ complex, further confirming apoptosis of A549 cells (Figure 3c). So it may be considered that the $[\text{Pd}^{\text{II}}(\text{L})\text{Cl}]$ complex induces apoptosis on A549 cells through the mitochondrial pathway, although further verification is needed.

Cancer chemotherapy is known to induce tumour cell death in a variety of cell types in part by promoting the production of intracellular ROS. In order to know whether ROS production is associated with $[\text{Pd}^{\text{II}}(\text{L})\text{Cl}]$, **1a** complex-induced apoptosis of A549 cells, we assessed the expression of ROS at respective concentrations of $[\text{Pd}^{\text{II}}(\text{L})\text{Cl}]$, **1a** complex treatment by examining the fluorescence intensity of DCHF-DA-incubated cells. Upon challenge of A549 cells for 24 h with $[\text{Pd}^{\text{II}}(\text{L})\text{Cl}]$, **1a**, a concentration-dependent increase of ROS production was observed (Figure 4). A representative fluorescence pattern from flow cytometry shows that the intracellular ROS level increased after $[\text{Pd}^{\text{II}}(\text{L})\text{Cl}]$, **1a** complex treatment in a dose-dependent manner (Figure 4a). Mean fluorescence intensity of untreated cells was $\sim 10\%$, and the values changed to $\sim 50\%$ and $\sim 70\%$, after treatment with 5 and 10 μM $[\text{Pd}^{\text{II}}(\text{L})\text{Cl}]$, **1a** respectively. Fluorescence

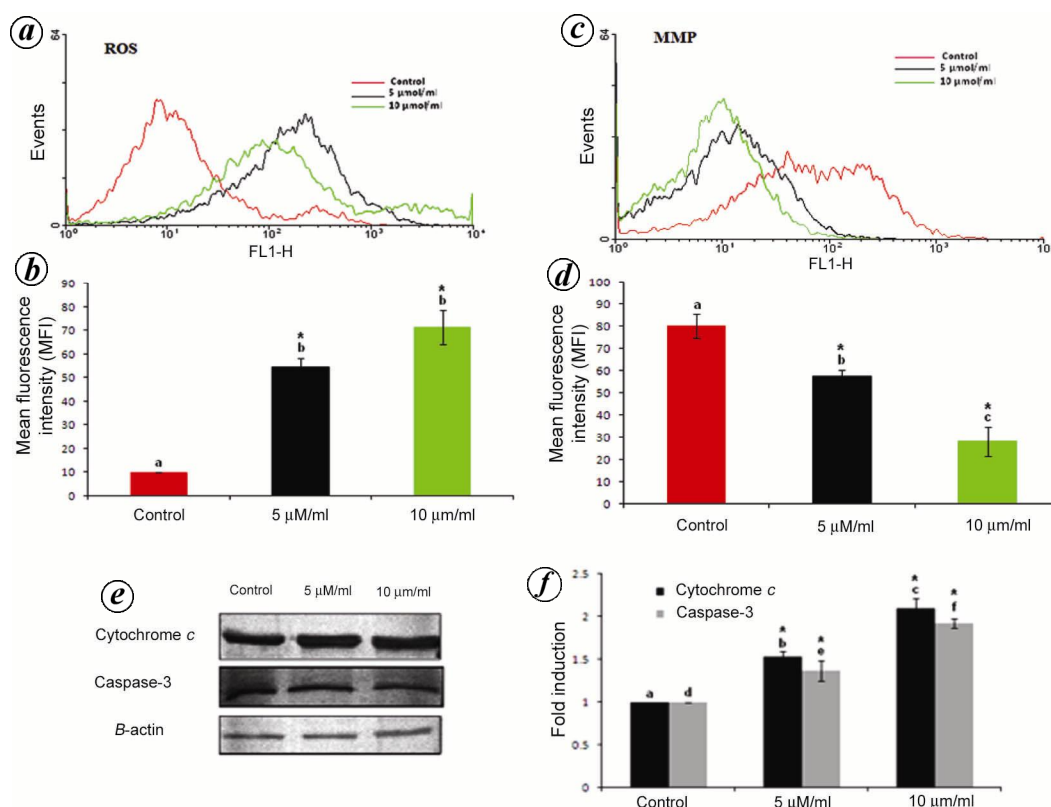


Figure 4. Flow cytometric analysis of $[\text{Pd}^{\text{II}}(\text{L})\text{Cl}]_1\mathbf{1a}$ induced reactive oxygen species production in A549 cells. Cells were harvested and when were 80% confluent they were treated with 0, 5 and 10 μM $[\text{Pd}^{\text{II}}(\text{L})\text{Cl}]_1\mathbf{1a}$ respectively, for 24 h. **a**, After treatment the cells were incubated with 20,70-dichlorofluorescein diacetate fluorescent probes and analysed by flow cytometry in a single labelling system with a 530-nm band pass filter using an overlay histogram plot. **b**, Bar graph represents the mean fluorescence intensity (MFI) compared with the control. Results are a single representative of five comparable experiments. Asterisks (*) indicates significant differences ($P < 0.05$, ANOVA followed by post hoc LSD test) in values for different doses compared to control. The different letters indicate significant differences ($P < 0.05$) between groups. **c**, Flow cytometric analysis of mitochondrial transition pore formation in response to $[\text{Pd}^{\text{II}}(\text{L})\text{Cl}]_1\mathbf{1a}$ treatment with 0, 5 and 10 μM $[\text{Pd}^{\text{II}}(\text{L})\text{Cl}]_1\mathbf{1a}$ respectively, for 24 h. The mitochondrial membrane permeability was measured by flow cytometry in a single labelling system using DiOC6 fluorescent probes and a 530 nm band-pass filter. The loss of fluorescence indicates the disintegration of mitochondrial membrane. **d**, Bar graph represents the MFI compared with the control. Results are a single representative of five comparable experiments. Asterisks (*) indicates significant differences ($P < 0.05$, ANOVA followed by post hoc LSD test) in values for different doses compared to control. The different letters indicate significant differences ($P < 0.05$) between groups. **e**, Effect of $[\text{Pd}^{\text{II}}(\text{L})\text{Cl}]_1\mathbf{1a}$ on cytochrome *c* and caspase-3 expression in A549 cells. The protein levels of apoptosis regulatory molecules, including cytochrome *c* and caspase-3 in A549 cells treated with $[\text{Pd}^{\text{II}}(\text{L})\text{Cl}]_1\mathbf{1a}$ at indicated concentrations for 24 h were analysed by Western blot assay. **f**, Bars represent quantitative densitometric values of the expressed protein in the samples shown in (e); β -actin used as loading control. Data shown are representative of five comparable experiments. Asterisks (*) indicates significant differences ($P < 0.05$, ANOVA followed by post hoc LSD test) in values for different doses compared to control. The different letters indicate significant differences ($P < 0.05$) between groups.

intensities of $[\text{Pd}^{\text{II}}(\text{L})\text{Cl}]_1\mathbf{1a}$ treated A549 cells were much higher than those of untreated controls ($P < 0.05$) (Figure 4 *a* and *b*).

To further demonstrate the induction of apoptosis by $[\text{Pd}^{\text{II}}(\text{L})\text{Cl}]_1\mathbf{1a}$ complex, the mitochondrial membrane depolarization was examined using DiOC₆. The A549 cells were treated with $[\text{Pd}^{\text{II}}(\text{L})\text{Cl}]_1\mathbf{1a}$ complex at a concentration of 5 and 10 μM for 24 h (Figure 4). Our results indicate that the $[\text{Pd}^{\text{II}}(\text{L})\text{Cl}]_1\mathbf{1a}$ complex induced mitochondrial membrane depolarization in a dose-dependent manner. These results clearly show that $[\text{Pd}^{\text{II}}(\text{L})\text{Cl}]_1\mathbf{1a}$ complex is an efficient inducer of mitochondrial

membrane depolarization of A549 cells. Since decreased DiOC₆ fluorescence is a measure of the integrity of the mitochondrial membrane, therefore the results from this study indicate decrease in integrity of the mitochondrial membrane after addition of $[\text{Pd}^{\text{II}}(\text{L})\text{Cl}]_1\mathbf{1a}$ at doses of 5 and 10 μM (Figure 4 *c* and *d*).

To understand the further downstream events of apoptosis, we examined whether the complex $\mathbf{1a}$ has any effect on the expressions of pro-apoptotic proteins cytochrome *c* and caspase-3. It is known that cytochrome *c* causes activation of caspases by cleaving the procaspases. Using Western blot analysis, we observed increased expression

of cytochrome *c* and caspase-3 (Figure 4), which signifies caspase-3 upregulation in treated A549 cells in comparison to the untreated ones. Therefore, increase in cytochrome *c* expression in the cell lysate suggests that [Pd^{II}(L)Cl], **1a** complex, upregulates caspase-3 to initiate the apoptotic cell death (Figure 4 *e* and *f*).

The search for new chemo-preventive and antitumour agents that are more effective but less toxic has become a matter of interest. Different palladium complexes with promising activity against varying kinds of tumour cell lines have been synthesized and tested over years^{30–34}. Taking into account the promising activity of palladium complexes against cancer, we have recently synthesized the [Pd^{II}(L)Cl], **1a** complex which shows cytotoxic effect with prostate cancer (PC-3) cells, modulating the cell cycle as well as the balance between pro- and anti-apoptotic proteins²⁹. In the present study, we first examined the anti-proliferative effect of [Pd^{II}(L)Cl], **1a** complex on human non-small lung cancer cells at concentrations ranging from 0 to 25 μM for 24 h. The [Pd^{II}(L)Cl], **1a** complex significantly decreased the proliferation of A549 cells in a dose and time-dependent manner. This was consistent with previous reports that daidzein inhibits the growth of human colon, breast, and ovarian carcinoma cells³⁵. Similar to the results of the cell proliferation experiment by trypan blue exclusion, the phase contrast photomicrographs of A549 cells treated with the [Pd^{II}(L)Cl], **1a** complex in different concentrations ranging from 0 to 25 μM for 24 h confirms the cell death of A549 cells with complex treatment.

Cell cycle control is a major event in cellular division. Blockade of the cell cycle is now considered as an effective strategy for the development of novel cancer therapies^{36,37}. To further scrutinize these results, we analysed cell cycle pattern of A549 cells treated with 0, 5 and 10 μM concentrations of [Pd^{II}(L)Cl], **1a** complex for 24 h. In the case of 10 μM treated A549 cells, the sub G0/G1 cell population increases (~27%) with respect to control (~3). As another measure of apoptosis, we determined the induction of apoptosis by examining the morphological change of nucleus by acridine orange staining method. The A549 cells treated with 10 μM [Pd^{II}(L)Cl], **1a** complex show a condensed nuclei compared to the control, which shows the intact nuclear architecture. Apoptosis is characterized with morphological and biochemical changes that include blebbing of the cell membrane, a decrease in cell volume, nuclear condensation and the intra-nucleosomal cleavage of DNA. In the phase contrast photomicrograph, we observed decrease in cell volume of A549 cells and also nuclear condensation by AO staining after treatment with [Pd^{II}(L)Cl], **1a** complex compared to control A549 cells. Both these experiment confirm the apoptosis of A549 cells induced by [Pd^{II}(L)Cl], **1a** complex.

The cell cycle arrest may partly explain apoptosis and anti-proliferative effects induced by [Pd^{II}(L)Cl], **1a**.

Apoptosis plays an important role in anti-cancer effect. It is a highly regulated death process by which cells undergo inducible non-necrotic cellular suicide³⁸. Data obtained from annexin V staining showed that [Pd^{II}(L)Cl], **1a** complex induces significant apoptosis in A549 cells. In this study, we observed that [Pd^{II}(L)Cl], **1a** also acts effectively on human lung cancer cells to induce cytotoxicity in a manner that causes apoptosis. Investigating the mechanism by which lung cancer cells undergo apoptosis in response to [Pd^{II}(L)Cl], **1a** treatment, we found that [Pd^{II}(L)Cl], **1a** treatment resulted in severe ROS accumulation. Excessive ROS caused oxidative damage to the mitochondrial membranes and impaired the membrane integrity, leading to cytochrome *c* release, caspase activation and apoptosis.

We have demonstrated that the cause of induced apoptosis is ROS. The generation of ROS in A549 cells was detected by DCFDA. ROS, such as H₂O₂ and O₂^{•-}, are constantly produced during metabolic processes in all living species. Under physiological conditions, the maintenance of an appropriate level of intracellular ROS is important in keeping redox balance and cell proliferation^{39–42}. Previously it was reported that cancer chemo-preventive agents induce apoptosis in part through ROS generation and disruption of redox homeostasis⁴³. It is also known that the pro-apoptotic signal(s) emanating from accumulated ROS trigger the mitochondrial release of caspase-activating proteins, such as cytochrome *c*, apoptosis inducing factor, and Smac/DIABLO to the cytosol⁴⁴. ROS shows secondary messenger function because of its ability to influence MMP and mitochondrial function and to induce intracellular Ca²⁺ flux and eventual activation of the caspase cascade⁴⁵.

One of the early events that initiate apoptosis is the release of cytochrome *c* from the mitochondria into the cytosol²⁹. Consistent with these results, in the cytosol of [Pd^{II}(L)Cl], **1a** treated A549 cells, cytochrome *c* was detected after a 24 h treatment. This complex activates caspase-9, which in turn cleaves and thereby activates caspase-3. In the [Pd^{II}(L)Cl], **1a** treated cells, release of cytochrome *c* from the mitochondria was followed by activation of caspase-3. Mitochondria are important in energy production, cellular calcium homeostasis, generation of ROS and capacity to release apoptogenic proteins⁴⁶. Several factors can stimulate mitochondria-mediated apoptosis; these include DNA damaging agents, UV, activation of tumour suppressors, and chemotherapeutic agents^{47–49}. Previously, it has been reported that the release of cytochrome *c* appeared to be dependent on the induction of mitochondrial permeability transition, which is associated with a decrease in mitochondrial transmembrane potential that results from the opening of PTP⁵⁰.

It has been reported that Bcl XL is down-regulated by cytochrome *c* protein^{22,23}. Since we observed an increase in cytochrome *c* expression, the role of cytochrome *c* in the down regulation of Bcl XL can be postulated. Bcl XL

is an anti-apoptotic gene and hence its down-regulation is associated with apoptosis induced by curcumin^{24,25}. In summary, we have demonstrated that [Pd^{II}(L)Cl], **1a** induces ROS-mediated apoptosis in A549 lung cancer cell lines, initiated upstream of mitochondrial dysfunction. A determining event that commits the cancer cells to apoptotic death subsequent to the loss of MMP, cytosolic release of cytochrome *c* and activation of the caspase cascade, further investigation would possibly develop [Pd^{II}(L)Cl], **1a** into a chemotherapeutic agent.

- Schiller, J. H., Harrington, D., Belani, C. P., Langer, C., Sandler, A. and Krook, J., Comparison of four chemotherapy regimens for advanced non-small-cell lung cancer. *N. Engl. J. Med.*, 2002, **346**, 92–98.
- Rosenberg, B., VanCamp, L., Trosko, J. E. and Mansour, V. H., Platinum compounds: a new class of potent antitumour agents. *Nature*, 1969, **222**, 385–386.
- O'Dwyer, P. J., Stevenson, P. and Johnson, S. W., Clinical status of cisplatin, carboplatin, and other platinum-based antitumour drugs. *Ver. Helv. Chim. Acta*, 1999, 31–72.
- Bear, J. L. *et al.*, Interaction of rhodium(II) carboxylates with molecules of biologic importance. *Cancer Chemother. Rep.*, 1975, **159**, 611–620.
- Giraldi, S., Sava, G., Bertoli, G., Mestroni, G. and Zassinovich, G., Antitumour action of two rhodium and ruthenium complexes in comparison with *cis*-diamminedichloro platinum(II). *Cancer Res.*, 1997, **37**, 2662–2666.
- Graham, R. D. and Williams, D. R., The synthesis and screening for anti-bacterial, -cancer, -fungicidal and -viral activities of some complexes of palladium and nickel. *J. Inorg. Nucl. Chem.*, 1979, **41**, 1245–1249.
- Tusek-Bozic, L., Juribasic, M., Traldi, P., Scarcia, V. and Furlani, A., Synthesis, characterization and antitumour activity of palladium(II) complexes of monoethyl 8-quinolylmethyl phosphonate. *Polyhedron*, 2008, **27**, 1317–1328.
- Kuduk-Jaworska, J., Puszko, A., Kibiak, M. and Pelczynska, M., Synthesis, structural, physico-chemical and biological properties of new palladium(II) complexes with 2,6-dimethyl-4-nitropyridine. *J. Inorg. Biochem.*, 2004, **98**, 1447–1456.
- Matesanz, A. I. and Souza, P., Novel cyclopalladated and coordination palladium and platinum complexes derived from alpha-diphenyl ethanedione bis (thiosemicarbazones): structural studies and cytotoxic activity against human A2780 and A2780 cisR carcinoma cell lines. *J. Inorg. Biochem.*, 2007, **101**, 1354–1361.
- Rebolledo, A. P. *et al.*, Palladium(II) complexes of 2-benzoylpyridine-derived thiosemicarbazones: spectral characterization, structural studies and cytotoxic activity. *J. Inorg. Biochem.*, 2005, **99**, 698–706.
- Padhye, S., Afrasiabi, Z., Sinn, E., Fok, J., Mehta, K. and Rath, N., Antitumour metallothiosemicarbazones: structure and antitumour activity of palladium complex of phenanthrenequinone thiosemicarbazone. *Inorg. Chem.*, 2005, **44**, 1154–1160.
- Pérez-Cabré, M. *et al.*, Pd(II) and Pt(II) complexes with aromatic diamines: study of their interaction with DNA. *J. Inorg. Biochem.*, 2004, **98**, 510–521.
- Matesanz, A. I., Perez, J. M., Navarro, P., Moreno, J. M., Colacio, E. and Souza, P., Synthesis and characterization of novel palladium(II) complexes of bis(thiosemicarbazone). Structure, cytotoxic activity and DNA binding of Pd(II)-benzyl bis(thiosemicarbazone). *J. Inorg. Biochem.*, 1999, **76**, 29–37.
- Tusek-Bozic, L., Furlani, A., Scarcia, V., De Clercq, E. and Balzarini, J., Spectroscopic and biological properties of palladium(II) complexes of ethyl 2-quinolyl methylphosphonate. *J. Inorg. Biochem.*, 1998, **72**, 201–210.
- Gao, E., Liu, C., Zhu, M., Lin, H., Wu, Q. and Liu, L., Current development of Pd(II) complexes as potential antitumour agents. *Anticancer Agents Med. Chem.*, 2009, **9**, 356–368.
- Divsalar, A., Saboury, A.A., Mansoori-Torshizi, H. and Ahmad, F., Design, synthesis, and biological evaluation of a new palladium(II) complex: beta-lactoglobulin and K562 as targets. *J. Phys. Chem. B*, 2010, **114**, 3639–3647.
- Dodoff, N. I. *et al.*, Structure, NMR spectra and cytotoxic effect of palladium(II) and platinum(II) complexes of glyoxylic acid oxime. *Chemija*, 2009, **20**, 208–217.
- Abu-Surrah, A. S., Al-Sa'doni, H. H. and Abdalla, M. Y., Palladium-based chemotherapeutic agents: routes toward complexes with good antitumour activity. *Cancer Ther.*, 2008, **6**, 1–10.
- Garoufis, A., Hadjikakou, S. K. and Hadjiliadis, N., Palladium coordination compounds as anti-viral, anti-fungal, anti-microbial and antitumour agents. *Coord. Chem. Rev.*, 2009, **253**, 1384–1397.
- Ray, S. *et al.*, Anticancer and antimicrobial metallopharmaceutical agents based on palladium, gold, and silver N-heterocyclic carbene complexes. *J. Am. Chem. Soc.*, 2007, **129**, 15042–15053.
- Hernández, W. *et al.*, Synthesis, characterization, and *in vitro* cytotoxic activities of benzaldehyde thiosemicarbazone derivatives and their palladium(II) and platinum(II) complexes against various human tumour cell lines. *Bioinorg. Chem. Appl.*, 2008, **690952**, 19148285.
- Caires, A. C., Recent advances involving palladium (II) complexes for the cancer therapy. *Anticancer Agents Med. Chem.*, 2007, **7**, 484–491.
- Messere, A. *et al.*, Antiproliferative activity of Pt(II) and Pd(II) phosphine complexes with thymine and thymidine. *J. Inorg. Biochem.*, 2007, **101**, 254–260.
- Keter, F. K., Kanyanda, S., Lyantagaye, S. S., Darkwa, J., Rees, D. J. and Meyer, M., *In vitro* evaluation of dichloro-bis (pyrazole) palladium(II) and dichloro-bis (pyrazole) platinum(II) complexes as anticancer agents. *Cancer Chemother. Pharmacol.*, 2008, **63**, 127–138.
- Corbi, P. P., Cagnin, F., Sabeh, L. P., Massabni, A. C. and Costa-Neto, C. M., Synthesis, spectroscopic characterization and biological analysis of a new palladium(II) complex with methionine sulfoxide. *Spectrochim. Acta Mol. Biomol. Spectrosc.*, 2007, **66**, 1171–1174.
- Pucci, D. *et al.*, Bioactive fragments synergically involved in the design of new generation Pt(ii) and Pd(ii)-based anticancer compounds. *Dalton Trans.*, 2008, 5897–5904.
- Onoa, G. B., Moreno, V., Freisinger, E. and Lippert, B., Pd(II)- and Pt(II)-cimetidine complexes. Crystal structure of trans-[Pt(N,S-cimetidine)(2)]Cl₂·12H₂O. *J. Inorg. Biochem.*, 2002, **89**, 237–247.
- Akrivos, P. D., ChemInform abstract: recent studies in the coordination chemistry of heterocyclic thiones and thionates. *Coord. Chem. Rev.*, 2011, **213**, 181–210.
- Mukherjee, S., Chowdhury, S., Chattopadhyay, A. P. and Bhattacharya, A., Spectroscopic, cytotoxic and DFT studies of a luminescentpalladium(II) complex of a hydrazone ligand that induces apoptosis in human prostate cancer cells. *Inorg. Chim. Acta*, 2011, **373**, 40–46.
- Budzisz, E., Krajewska, U. and Rózalski, M., Cytotoxic and proapoptotic effects of new Pd(II) and Pt(II)-complexes with 3-ethanimidoyl-2-methoxy-2H-1, 2-benzoxaphosphinin-4-ol-2-oxide. *Pol. J. Pharmacol.*, 2004, **56**, 473–478.
- Ruiz, J. *et al.*, Palladium(II) and platinum(II) organometallic complexes with 4,7-dihydro-5-methyl-7-oxo[1, 2, 4]triazolo [1,5-a]pyrimidine. Antitumour activity of the platinum compounds. *Inorg. Chem.*, 2008, **47**, 4490–4505.
- Eryazici, I., MooreWeld, C. N. and Newkome, G. R., Square-planar Pd(II), Pt(II), and Au(III) terpyridine complexes: their syntheses, physical properties, supramolecular constructs, and biomedical activities. *Chem. Rev.*, 2008, **108**, 1834–1895.

33. Al-Masoudi, N. A., Abdullah, B. H., Essa, A. H., Loddo, R. and LaColla, P., Platinum and palladium–triazole complexes as highly potential antitumour agents. *Arch. Pharm. (Weinheim.)*, 2010, **343**, 222–227.
34. Tamasi, G. *et al.*, New platinum–oxicam complexes as anti-cancer drugs. Synthesis, characterization, release studies from smart hydrogels, evaluation of reactivity with selected proteins and cytotoxic activity *in vitro*. *J. Inorg. Biochem.*, 2010, **104**, 799–814.
35. Shaheen, F., Badshah, A., Gielen, M., Gieck, C., Jamil, M. and de Vos, D., Synthesis, characterization, *in vitro* cytotoxicity and anti-inflammatory activity of palladium(II) complexes with tertiary phosphines and heterocyclic thiolates: crystal structure of [Pd₂(C₂₈H₁₉N₈P₂)₂]. *J. Organomet. Chem.*, 2008, **693**, 1117–1126.
36. Buolamwini, J. K., Cell cycle molecular targets in novel anticancer drug discovery. *Curr. Pharm. Des.*, 2000, **6**, 379–392.
37. McDonald, E. R. and El-Deiry, W. S., Cell cycle control as a basis for cancer drug development. *Int. J. Oncol.*, 2000, **16**, 871–886.
38. Kaufmann, S. H. and Hengartner, M. O., Programmed cell death: alive and well in the new millennium. *Trends. Cell Biol.*, 2011, **111**, 526–534.
39. Chin, M. Y., Ng, K. C. and Li, G., The novel tumour suppressor p33ING2 enhances UVB-induced apoptosis in human melanoma cells. *Exp. Cell Res.*, 2005, **304**, 531–543.
40. Rotem, R., Heyfets, A., Fingrut, O., Blickstein, D., Shaklai, M. and Flescher, E., Jasmonates: novel anticancer agents acting directly and selectively on human cancer cell mitochondria. *Cancer Res.*, 2005, **65**, 1984–1993.
41. Bradham, C. A., Qian, T., Streetz, K., Trautwein, C., Brenner, D. A. and Lemasters, J. J., The mitochondrial permeability transition is required for tumour necrosis factor alpha-mediated apoptosis and cytochrome *c* release. *Mol. Cell. Biol.*, 1998, **18**, 6353–6364.
42. Preeta, R. and Nair, R. R., Stimulation of cardiac fibroblast proliferation by cerium: a superoxide anion-mediated response. *J. Mol. Cell. Cardiol.*, 1999, **31**, 1573–1580.
43. Murrell, G. A., Francis, M. J. and Bromley, L., Modulation of fibroblast proliferation by oxygen free radicals. *Biochem. J.*, 1990, **265**, 659–665.
44. Nicotera, T. M., Privalle, C., Wang, T. C., Oshimura, M. and Barrett, J. C., Differential proliferative responses of Syrian hamster embryo fibroblasts to paraquat generated superoxide radicals depending on tumour suppressor gene function. *Cancer Res.*, 1994, **54**, 3884–3888.
45. Martin, K. R. and Barrett, J. C., Reactive oxygen species as double-edged swords in cellular processes: low-dose cell signalling versus high-dose toxicity. *Hum. Exp. Toxicol.*, 2002, **21**, 71–75.
46. Petit, P. X., Lecoecur, H., Zorn, E., Dauguet, C., Mignotte, B. and Gougeon, M. L., Alterations in mitochondrial structure and function are early events of dexamethasone-induced thymocyte apoptosis. *J. Cell Biol.*, 1995, **130**, 157–167.
47. Li, P. *et al.*, Cytochrome *c* and dATP dependent formation of Apaf-1/caspase-9 complex initiates an apoptotic protease cascade. *Cell*, 1997, **14**, 479–489.
48. Brookes, P. S., Yoon, Y., Robotham, J. L., Anders, M. W. and Sheu, S. S., Calcium, ATP, and ROS: a mitochondrial love–hate triangle. *Am. J. Physiol. Cell. Physiol.*, 2004, **287**, 817–833.
49. Brookes, P. S., Mitochondrial proton leak and superoxide generation: an hypothesis. *Biochem. Soc. Trans.*, 1998, **26**, S331.
50. Cai, S., Xu, Y., Cooper, R. J., Ferkowicz, M. J., Hartwell, J. R. and Pollok, K. E., Mitochondrial targeting of human O6-methylguanine DNA methyl transferase protects against cell killing by chemotherapeutic alkylating agents. *Cancer Res.*, 2005, **65**, 3319–3327.

ACKNOWLEDGEMENTS. We thank Dr Suman Sengupta and Mr Samir Jana for cell culture maintenance and providing information on different techniques applied.

Received 3 October 2013; revised accepted 23 July 2014

Measuring the impacts of land use on water quality influenced by non-point sources

Ranen Sen^{1,2,*}, Sharadindra Chakrabarti² and Somdatta Chakravorty³

¹Formerly at Department of Metallurgical Engineering, Colorado School of Mines, USA

²Department of Applied Geology and Environment Systems Management, Presidency University, Kolkata 700 073, India

³Department of Computer Science & Engineering and Information Technology, Government College of Engineering and Ceramic Technology, Kolkata 700 010, India

The objective of this study is to (a) test the proposition that the variance of water quality from undefined sources is a function of land use within the watershed, and (b) examine the premise that the impact of land use near the stream is more important than that far away from the stream in affecting the water quality from non-point sources. Results obtained using this approach support both these hypotheses. Moreover, these tests suggest the importance of considering the means by which chemical elements are delivered to the streams. Nitrate-nitrogen and phosphorus can probably be intercepted by different means because of their varying delivery systems. Nitrate-nitrogen can be intercepted by removal of fast-growing floodplain crops and phosphorus by sediment barriers at sites outside the floodplain. Further evidences suggest that reservoir trap-efficiency is considerably important in improving the downstream water quality as the former entraps clay nanominerals (with adsorbed particulates of phosphorus) that are found to be responsible for the fate and transport of phosphorus. The methodology of analysis of stream loads is ordinary least square regression analysis. Stream loads of nitrate-nitrogen and total phosphorus have been studied as a function of land use.

Keywords: Land use, non-point source, nitrate-nitrogen, phosphorus, water quality.

THE primary objective of a non-point source (NPS) pollution control watershed project is to protect or restore the designated use of a water resource by reducing pollutant delivery to it. Because NPS of pollution is usually widespread, intermittent and undefined, mitigating a water quality problem, or potential problem, caused by such pollution is often difficult. The task is further complicated when sufficient time and funding are not available to implement all the recommended best management practices (BMPs). For this reason, a land treatment or watershed management strategy should be developed to guide the selection and implementation of BMPs. While

*For correspondence. (e-mail: rnarayansen@rediffmail.com)